Autonomous and Battery-Free Wireless Tag combining UWB and BLE Technology

Alassane Sidibe, Mohamed Abo Kassem, Alexandru Takacs, Jan Mennekens, Julien Dachy

Autonomous and Battery-Free Wireless Tag combining UWB and BLE Technology

Alassane SIDIBE
LAAS-CNRS, UWINLOC
Université de Toulouse, CNRS
Toulouse, FRANCE
alassane.sidibe@laas.fr

Mohamed ABO KASSEM
LAAS-CNRS
Université de Toulouse, CNRS
Toulouse, FRANCE
mohamed.abokassem@laas.fr

Alexandru TAKACS
LAAS-CNRS
Université de Toulouse, CNRS, UPS
Toulouse, FRANCE
alexandru.takacs@laas.fr

Jan MENNEKENS
Uwinloc
Toulouse, FRANCE
jan@uwinloc.com

Julien DACHY
Uwinloc
Toulouse, FRANCE
julien.dachy@uwinloc.com

***Abstract*— This paper presents a multifunctional, battery-free tag combining Bluetooth Low Energy (BLE) and Ultra-Wideband (UWB) technology powered by the far-field wireless power transmission technique. The proposed tag, with a size of 9 x 8 cm², can be used for asset tracking via UWB at a center frequency of 4 GHz or for wireless temperature and humidity monitoring via BLE at 2.45 GHz. The tag is powered by a highly efficient radiofrequency (RF) energy harvesting (EH) solution at 868 MHz. The proposed solution has been optimised for low power consumption of 5-15 µJ (for a single UWB transmission) and can provide reliable performance in terms of data sensing and geolocation at a low ambient power density. The electronic module that includes the features of the energy harvester (rectifier) and the UWB transceiver was previously developed by Uwinloc. Simulation results for both antennas (UWB and RF EH) were presented. The transmission rate in BLE and UWB configuration was also evaluated as a function of the EIRP power level.**

***Keywords*—Energy harvesting, Wireless power transmission, sensors, Ultra-wideband technology, Bluetooth low energy, Localisation, UHF antennas.**

I. Introduction

The development of low-power wireless communication technologies has increased the use of the Internet of Things (IoT). In addition, we are faced with the need for monitoring and having the continuous position of a large volume of assets. Solutions are proposed to solve indoor location problems as presented in [1]. Ultra-Wideband (UWB) technology outperformed the current technologies used for geolocation (e.g. Bluetooth, WIFI and GPS [2]). It has the advantages of presenting a high-ranging accuracy, robustness to multipath effects and high refresh rates for real-time localisation, and is becoming a potential technology for daily life applications [3], [4]. It can also cover space applications in the tracking of floating objects inside space stations [5].

For long-range data transmission and low power consumption, BLE is the most suitable technology for sensor-based IoT applications [6]. However, most devices are battery operated and may sometimes deal with a limited lifetime and regular maintenance for battery replacement. Thus, for a longer lifetime, it may be necessary to harvest the energy by using far-field Wireless Power Transmission (WPT) [7].

Recent research activities have enabled the development of a battery-free system for sensing and data communication as in [8] for light-sensing through Bluetooth Low Energy (BLE) protocol. Other activities are more focused on finding a hybrid solution UWB/BLE tag for tracking elderly persons but is battery-powered [9].

The work in this paper is part of the needs of Uwinloc company which develops and commercialises an indoor location solution using a battery-free tag [10]. The commercialised tag is wirelessly powered by electromagnetic (EM) waves radiated by a Radiofrequency Identification (RFID) source at 868 MHz. For an accurate and reliable location, the tag emits a signal using UWB technology at centre frequency of 4 GHz.

To the authors' best knowledge, this paper proposes the first battery-free UWB/BLE tag with sensing (temperature & humidity) and localisation capabilities.

II. Architecture and Design of the Proposed Tag Prototype

The tag developed consists of a combination of a geolocation module (GM), enabling RF energy harvesting and UWB transmission for accurate location, a temperature/humidity sensor, and a BLE transceiver. It is powered wirelessly by a far-field WPT and uses a Power Management Unit (PMU) to boost, store (in a capacitor) and manage the available power from the harvester as seen in Fig. 1. The proposed solution has been prototyped on a 1.55 mm thick FR-4 substrate. Thanks to the jumper (J1), different combinations are possible to allow multiple functionalities of the tag:

(i) *The use of the tag for geolocation only in UWB mode*. In this mode, the harvested power (P_{out}) obtained at the output pin of the harvester is connected (by using the jumpers J1) to the input pin (V_{cc}) of the GM and other chips are disconnected. Humidity and temperature sensing are also possible by supplying the sensor with the right combination of jumper J1.

This first developed board does not yet allow simultaneously the geolocation through UWB and the BLE sensing. J2 is used for I2C communication either by the GM or by the BLE System on Chip (SoC).

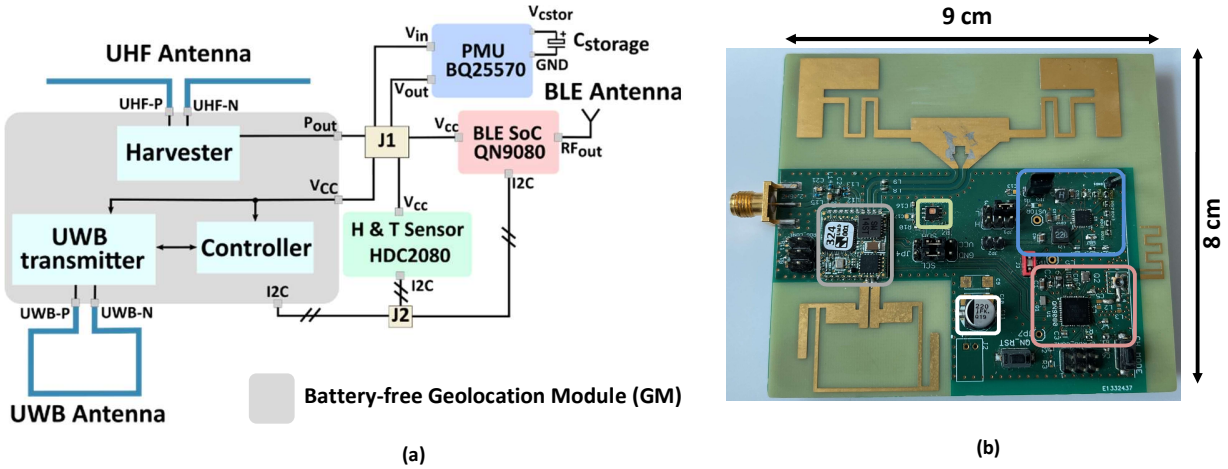

Fig. 1. (a) Architecture of the battery-free UWB-BLE tag; (b) Photo of prototyped tag.

(ii) *The use of the tag for temperature and humidity monitoring through BLE communication*. The harvested DC power is directly managed by the PMU and is stored in the capacitor. The BLE transceiver and active sensors are then supplied when there is sufficient energy available in the capacitor. The right combination on J1 allows this configuration.

A. Bluetooth Low Energy sensing and communication

For data transmission, we opted for the ultra-low-power BLE SoC from NXP [11] and a conventional meandered Planar Inverted-F Antenna (PIFA) designed at 2.4 GHz as suggested in the application note [12]. Knowing that the instantaneous power available from the harvester is not sufficient to supply the BLE transceiver and active sensors, we decided to use a storage capacitor of 220 µF and the BQ25570 as low-power PMU (its minimum input DC power is around 15 µW for 100 µF according to the datasheet) [13]. Its DC output voltage is chosen to 1.9 V to achieve the best compromise for low power consumption by the BLE transceiver and sensors. To save energy, the BLE transceiver is programmed to operate as a transmitter (broadcaster) only, sending the measured temperature and humidity data in advertising (Adv.) mode. A paper has examined the packed collision for BLE advertising mode [14]. The probability of packet collisions can be reduced by increasing the advertising time and number of packets at the expense of increasing the energy consumption. We found out a trade-off by sending 4 advertising events with an interval of 250 ms. Each advertising event is composed of 3 advertising packets over the 3 allocated channels (37, 38, and 39). The BLE advertisement profile can be obtained thanks to the QN9080 NPX development board via the power measurement tool of MCUXpresso IDE software as seen in Fig. 2.

The broadcasting phase begins from a sleep state with an inrush current followed by the initialisation and measurement of data and ends with a function (stop Adv). This function stops the timer used to periodic advertising after 4 times and also forces the discharge of the storage capacitor for another cycle.

The packets are sent to the observer which is a QN9080 NPX development board configured in observer mode [15]. An integrated low-power temperature and humidity sensor HDC2080 is chosen from Texas Instrument (TI) [16]. The operation of the sensor and the BLE SoC requires an energy consumption of about 756 µJ for 3 advertising events and 942 µJ for the broadcasting phase. The PMU is configured to have a minimum and maximum DC voltage thresholds at 1.97 V and 3.55 V, respectively. The storage capacitor ($C_{storage}$), EEEFK0J221P from Panasonic was carefully chosen to be 220 µF, to store the sufficient energy for the active components and to allow a low leakage current [17]. Thus, the maximum energy stored by the capacitor is about 1.39 mJ during the first charge (cold start phase) from an empty state ($V_{storage}$ = 0 V) to maximum voltage allowed by the PMU ($V_{storage}$ = 3.55 V) and 960 µJ during each subsequent recharge (before each sensing and data transmission). During these recharges, the minimum voltage allowed at the output of the capacitor before the advertising stop is set at 1.97 V.

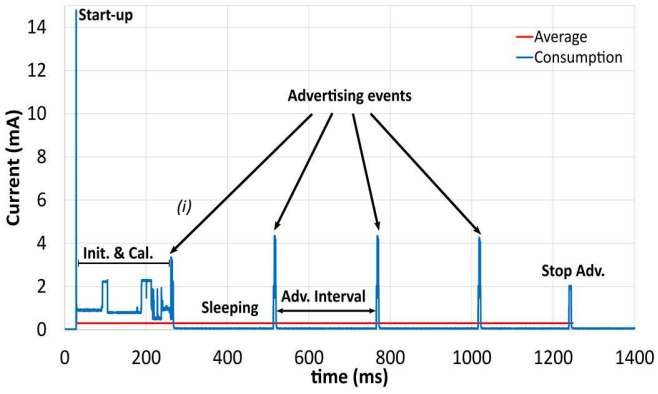

Fig. 2. Current consumption of the tag configured in BLE mode: the average value (red) and the evolution as function of the time of the current (blue) during the broadcasting time.

B. *Harvester and Ultra-Wideband Module*

The battery-free geolocation module developed by Uwinloc company, allows the real-time tracking of assets.

The GM was developed to allow two differential inputs for the energy harvesting features. One is used for the proposed solution and the other is connected to an SMA connector for additional experimentation (not reported in this paper). The harvester is based on Greinacher doubler topology optimised for low-power density available from a dedicated RF energy source operating in the Industrial Scientific Medical (ISM) frequency band at 868 MHz. To achieve this, the power consumption of the GM module has been significantly reduced by minimising the power required by the microcontroller, the transmitter as well as the leakage current of the first storage capacitor (60 µF included in the harvester block, see Fig. 1b) for UWB operation. More details about the energy harvesting circuit can be found in the patent [18]. The GM needs about 5 to 10 µJ for a single UWB transmission. Once enough energy is stored, the tag transmits an ultra-wideband pulse through the UWB antenna to UWB beacons (not presented in this paper). The 3-Dimensional (3D) position of the tag is accurately computed thanks to triangulation algorithm.

The design of the antenna is particularly important to achieve the best compromise in terms of high sensitivity at low power density to be received, UWB transmission range, and accuracy for localisation. To avoid additional lumped components and thus insertion losses, UWB and Ultra High Frequency (UHF) antennas have been designed to have an impedance that is the complex conjugate of the input impedance of the UWB transmitter ($25 - j \cdot 9\ \Omega$) and harvester ($30 - j \cdot 250\ \Omega$). The UHF antenna (used for energy receiving) consists of a modified folded dipole antenna based on a T-match structure at 868 MHz. The high value of the imaginary part of the input impedance of GM is compensated by the Coplanar Wave Guided Grounded (CPWG) coupled transmission lines.

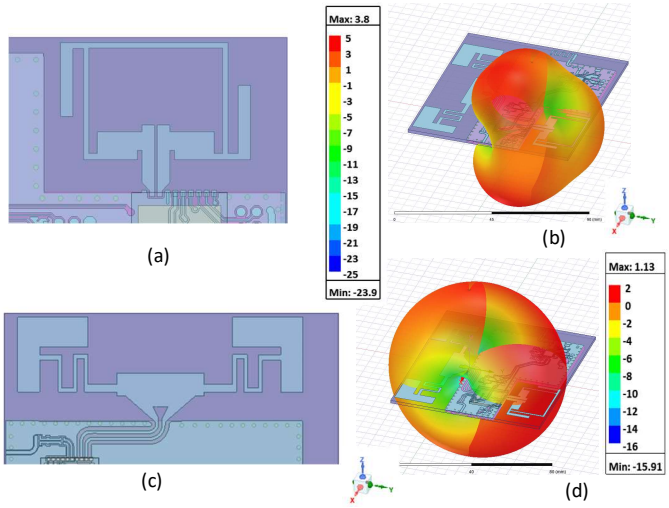

Fig. 3. Antenna design and simulation of the tag: (a) Proposed design of the UWB antenna; (b) 3D Radiation pattern of the UWB antenna at 4 GHz; (c) Proposed design of the UHF antenna; (d) 3D Radiation pattern of the UHF antenna at 868 MHz.

The maximum simulated gain at the desired frequency is around +1.13 dBm for the theta angle equal to 90° in the YoZ plane (Phi = 90°) which will correspond to the horizontal position (H-pos) for the experiments. The vertical position (V-pos) will also correspond to the orientation in which the antenna has a gain of 0 dBi at theta equal to 0° in the YoZ plan as presented in Fig. 2.

The UWB antenna is based on a novel modified loop antenna to have a wideband behavior (Fig. 2 (a)). However, the presence of the UHF antenna and the wider ground plane, have modified the radiation pattern to be more directional in a certain direction. The two crossed arms at the corner of the loop are used to improve the radiation pattern of the antenna. According to the simulation, it has a maximum gain of +3.8 dBi at 4 GHz.

III. Experimental Results

A. *Bluetooth Low Energy Performances*

In this part, the tag was configured to operate with the harvester, PMU, sensors, and the BLE SoC. The prototyped tag (operating in BLE mode) was tested in an anechoic chamber with a dedicated RF source composed of a transmitting patch antenna (placed at a distance d about 2 meters from the tag under test) connected to an RF signal generator (Anritsu MG3694B) through a cable to provide the power P_{RF} at the frequency of 868 MHz. The losses due to the cable were accurately measured using a power meter and the average value is estimated to be -0.5 dB. The measurement setup is shown in Fig. 4. Prior to the measurements, all the capacitors are manually discharged to perform an accurate measurement of the time during the cold start phase. The BLE receiver operates as observer/listening device and is connected to a laptop. The QN9080 development kit is used to achieve this function. Next, the emission rate (i.e., the time elapsed between two consecutive temperature/humidity measurements sent by the battery-less tag through the advertising channels during the broadcasting phase) is evaluated by doing the time difference between each broadcasting phase. The time required for the cold start mode and the average emission rate as a function of the Effective Isotropic Radiated Power (EIRP) power of the RF source (placed at 2 meters from the tag) are shown in Fig. 5.

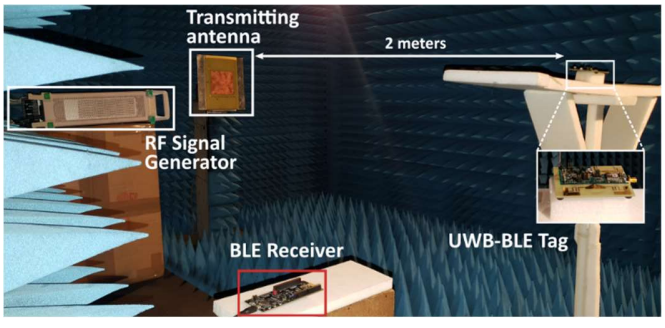

Fig. 4. BLE measurement setup of the tag in an anechoic chamber.

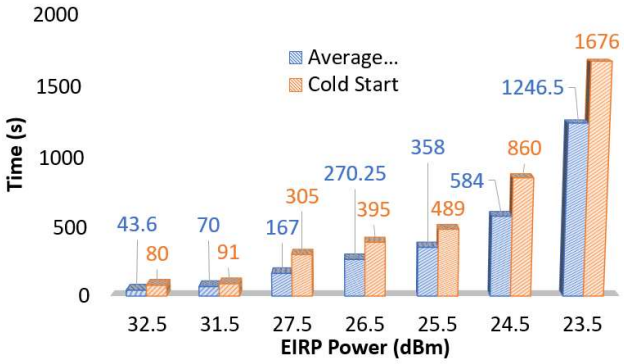

Fig. 5. Measured BLE emission rate and the time of the cold start phase as function of the EIRP power of the 868 MHz RF source located at 2 m far away the tag.

Knowing that the measurement was operated in an anechoic chamber without any reflection, the Friis formula in (1) enables the calculation of the received power at the output of the UHF antenna.

$$P_{rx(dB)} = P_{tx} + G_{tx} + G_{rx} + 20 \cdot \log_{10}\left(\frac{\lambda}{4 \cdot \pi \cdot D}\right) \qquad (1)$$

Since the transmitted power is greater than +23.5 dBm EIRP (corresponding to an estimated received power of -12.65 dBm at the input of the harvester) the cold start time is less than 28 minutes. By extrapolating with the formula (1), this result for a maximum EIRP power of +33 dBm, it is possible to estimate the maximum range around 6 meters for an average equivalent emission rate of 1246 seconds.

B. Ultra-Wideband Performances

The prototyped tag is now configured to work with the GM only for preliminary results. The evaluation of the emission rate was performed under the same conditions as the BLE part with the setup shown in Fig. 4, but the BLE receiver is replaced by a UWB beacon. In this case, two distinct positions of the tag were chosen. The horizontal position (H-pos) corresponds to the one used in the BLE tests and the vertical (V-pos) corresponds to the orientation in which the tag is placed vertically in front of the transmitting antenna. According to the simulation, the UHF antenna has less gain in the V-pos than in the H-pos. The maximum emission rate allowed for a given EIRP power was set at about 10 minutes (Fig. 6) to allow fast monitoring of the evolution of the tag location/position. Comparing the emission rate at each position, the time difference (tag in H-pos versus tag in V-pos) is larger at low power due to the nonlinearity of the harvester and the losses. By using the formula (1), we can estimate that an UWB emission is possible as far as the received RF power at the input of the rectifier is higher than -20 dBm. The UHF antenna of the tag at 868 MHz has a simulated gain of +1.13 dBi (in H-Pos) and the RF source with an EIRP of +18 dBm was located at 2 m far away from tag. Once UWB communication capability between tag and beacon is evaluated inside an anechoic chamber we have performed an experiment to evaluate the UWB localisation performances in a real scenario.

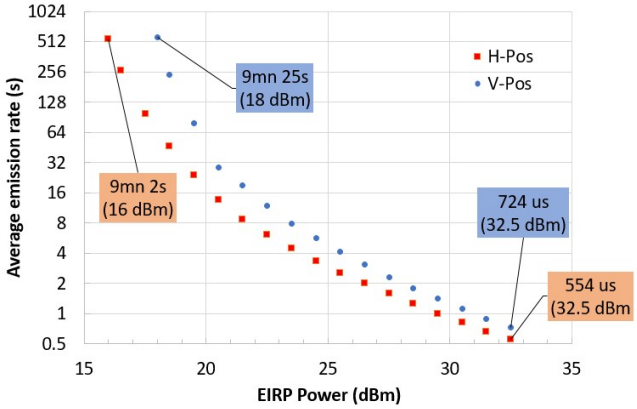

Fig. 6. Average emission rate of the tag in localisation mode without sensor.

For this purpose, an indoor test was conducted in a 300 m² test warehouse containing multiple obstructions from Uwinloc company. The configuration of the test area and the number of beacons are company specific and have not been adapted for the test in this paper. A detail about the method and device for the detection of the UWB pulse is presented in [19]. Two prototyped tags were placed separately in the test area as seen in Fig. 7. Energy sources were configured respecting the ESTI standard [20] with the continuous wave (CW) at the RFID frequency band with a power levels at 2 W. The beacons enabling to receive the UWB signal are placed in the corners and the facades of the test area at a height of 5-6 meters (whose coordinates are known) as shown in Fig. 8 (a). Among the 13 beacons configured, 11 of them have received the UWB signal. The location is then calculated by an algorithm to display the position on the software graphic interface developed by Uwinloc (Fig. 8 (b)).

This accuracy depends on the tag position in relation to the location of the beacons. Based on the tests available the date of submission, the position accuracy is lower than 1 m and this is strongly dependent on the tag position and orientation. The real-time position of the tags is obtained on the map by filtering its unique identification via the user interface. Works are in progress to evaluate the performance of the tag in a harsh environment by embedding it in a concrete beam and to also implement the sensing capability in UWB mode.

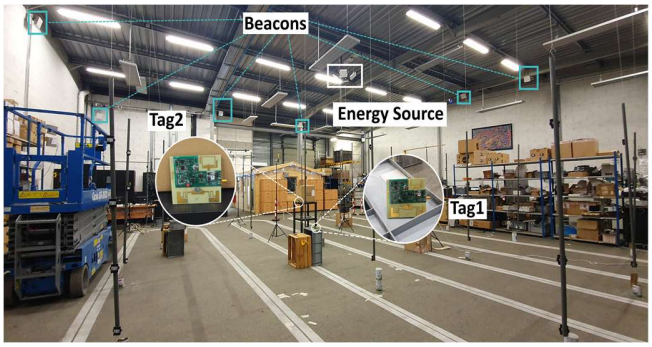

Fig. 7. Geolocation setup of the tags in the 300 m² test area. Thirteen beacons (only six are visible here) and two tags (placed at various position) have been used.

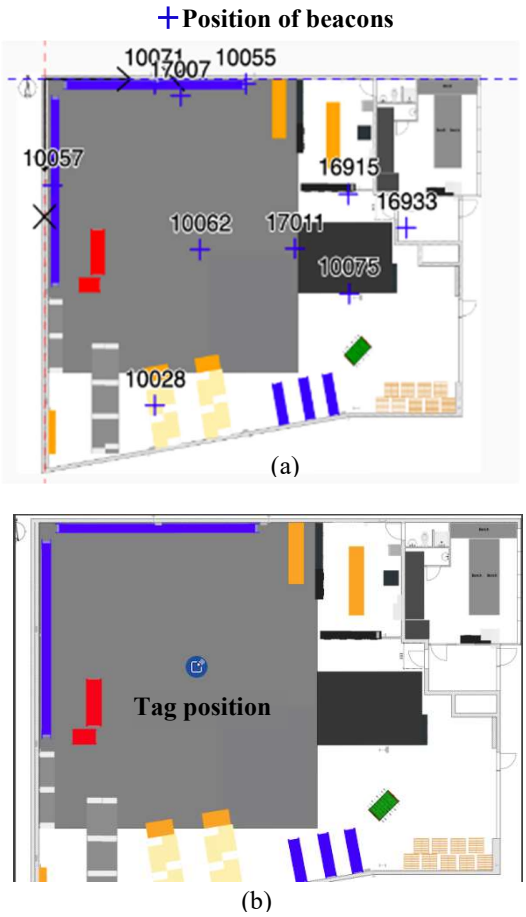

Fig. 8. (a) Mapping of the geolocation tag in the test area: each beacon (fixed position) is represented by its unique identification. (b) The position of the geolocated tag: only one tag was shown inside the overall volume of the test area (1800 m^3).

IV. Conclusion

This paper has presented for the first time a unique solution of a battery-free multifunction tag combining geolocation in UWB mode and wireless sensing in BLE mode. The prototyped tag is based on an electronic module developed by Uwinloc Company that enables RF EH and UWB transmission. The design has included UHF antenna at 868 MHz and UWB antenna at 4 GHz with a maximum simulated gain of +1.13 dBi and +3.8 dBi, respectively. The prototyped tag was first configured in BLE mode with sensors to evaluate its performance. As a function of the EIRP of the RF source, the measured cold start time was between 80 seconds (EIRP = +32.5 dBm) and 28 minutes (EIRP = +23.5 dBm) while the periodicity of sensing (that is identical with the BLE emission rate in advertising mode) was between 44 seconds (EIRP = +32.5 dBm) and 21 minutes (EIRP= +23.5 dBm). In UWB mode, the average emission rate was measured, and the tag was placed in a 300 m² indoor test area to have a preliminary estimation of the location precision. As confirmed by the experimental results, the location accuracy is lower than 1 m and strongly dependent of the tag position and the obstructions presented in the test area.

References

[1] 'Summary of available indoor location techniques - Google Scholar'. https://scholar.google.com/scholar?hl=fr&as_sdt=0%2C5&q=Summary+of+available+indoor+location+techniques&btnG= (accessed Apr. 28, 2022).

[2] 'ultrawideband.pdf', *Federal Communications Commission*. https://www.fcc.gov/files/ultrawidebandpdf (accessed Dec. 06, 2021).

[3] T. Feng, Y. Yu, L. Wu, Y. Bai, Z. Xiao, and Z. Lu, 'A human-tracking robot using ultra wideband technology', *IEEE Access*, vol. 6, pp. 42541–42550, 2018.

[4] G. Mokhtari, Q. Zhang, C. Hargrave, and J. C. Ralston, 'Non-wearable UWB sensor for human identification in smart home', *IEEE Sens. J.*, vol. 17, no. 11, pp. 3332–3340, 2017.

[5] D. Dardari *et al.*, 'An ultra-wideband battery-less positioning system for space applications', in *2019 IEEE International Conference on RFID Technology and Applications (RFID-TA)*, 2019, pp. 104–109.

[6] 'Bluetooth Technology Overview', *Bluetooth® Technology Website*. https://www.bluetooth.com/learn-about-bluetooth/tech-overview/ (accessed Dec. 06, 2021).

[7] H. J. Visser, H. W. Pflug, and S. Keyrouz, 'Far-Field Wireless Power Transfer for IoT Sensors', in *Wireless Power Transfer Algorithms, Technologies and Applications in Ad Hoc Communication Networks*, S. Nikoletseas, Y. Yang, and A. Georgiadis, Eds. Cham: Springer International Publishing, 2016, pp. 85–110. doi: 10.1007/978-3-319-46810-5_4.

[8] R. La Rosa, C. Dehollain, A. Burg, M. Costanza, and P. Livreri, 'An Energy-Autonomous Wireless Sensor with Simultaneous Energy Harvesting and Ambient Light Sensing', *IEEE Sens. J.*, 2021.

[9] J. Kolakowski, V. Djaja-Josko, M. Kolakowski, and K. Broczek, 'UWB/BLE tracking system for elderly people monitoring', *Sensors*, vol. 20, no. 6, p. 1574, 2020.

[10] 'UWINLOC | New Indoor Location System for assets tracking', *UWINLOC | Indoor Location System*. https://uwinloc.com/ (accessed Feb. 09, 2022).

[11] 'QN908x: Ultra-Low-Power Bluetooth Low Energy System on Chip (SoC) Solution | NXP Semiconductors'. https://www.nxp.com/products/wireless/bluetooth-low-energy/qn908x-ultra-low-power-bluetooth-low-energy-system-on-chip-solution:QN9080 (accessed Dec. 06, 2021).

[12] 'Compact Planar Antennas for 2.4 GHz Communication', p. 48.

[13] 'BQ25570 datasheet | TI.com'. https://www.ti.com/document-viewer/BQ25570/datasheet/revision-history-slusbh21212#SLUSBH21212 (accessed Dec. 06, 2021).

[14] M. Ghamari *et al.*, 'Detailed examination of a packet collision model for Bluetooth Low Energy advertising mode', *IEEE Access*, vol. 6, pp. 46066–46073, 2018.

[15] 'QN9080SIP Development Kit'. https://www.nxp.com/design/development-boards/freedom-development-boards/wireless-connectivy/a-highly-extensible-platform-for-application-development-of-qn9080sip:QN9080SIP-DK (accessed Feb. 14, 2022).

[16] 'HDC2080 datasheet | TI.com'. https://www.ti.com/document-viewer/HDC2080/datasheet/GUID-5AB554A1-5F5B-4CF8-B0D0-9590654E767A#TITLE-SNAS678SNAS6781218 (accessed Dec. 06, 2021).

[17] 'EEEFK0J221P - Aluminum Electrolytic Capacitors (Surface Mount Type) - Aluminum Electrolytic Capacitors - Industrial Devices & Solutions - Panasonic'. https://industrial.panasonic.com/ww/products/pt/aluminum-cap-smd/models/EEEFK0J221P (accessed Feb. 13, 2022).

[18] USPTO.report, 'Radio-frequency Energy Harvesting Circuit And Communication Device Integrating Such A Radio-frequency Energy Harvesting Circuit Patent Application', *USPTO.report*. https://uspto.report/patent/app/20210249901 (accessed Apr. 22, 2022).

[19] USPTO.report, 'Method And Device For The Detection Of A Pulse Of A Signal Patent Application', *USPTO.report*. https://uspto.report/patent/app/20200091956 (accessed Apr. 22, 2022).

[20] 'ETSI TR 102 436 V2.1.1 (2014-06) - Electromagnetic compatibility and Radio spectrum Matters (ERM); Short Range Devices (SRD) intended for operation in the bands 865 MHz to 868 MHz and 915 MHz to 921 MHz; Guidelines for the installation and commissioning of Radio

Frequency Identification (RFID) equipment at UHF', *iTeh Standards Store*. https://standards.iteh.ai/catalog/standards/etsi/8e50724b-db29-45ad-8e8b-d5681b109ee8/etsi-tr-102-436-v2-1-1-2014-06 (accessed Apr. 22, 2022).